Separation of Cellulose Nanocrystals from Bromelia (*Neoglaziovia variegate*) Fibers Using Ionic Liquids Based on Hydrogen Sulfate Anion

Ana Paula Bispo Gonçalves[1*], Emanoel Oliveira[2], Mariana Souza[2,3], Fábio Costa[3], Cleidiene Miranda[2], Paulo Romano Correia[4], Silvana Mattedi[3], Nadia José[2]

[1]SENAI CIMATEC University Center; [2]GECIM Research Group, Chemistry Institute Federal University of Bahia; [3]Chemical Engineering Graduate Program, Polytechnic School, Federal University of Bahia; [4]Departament of Biotechnology, Federal University of Bahia, Institute of Sciences of Health; Salvador, Bahia, Brazil

Due to the environmental appeal that has grown in recent years, the use of agricultural wastes and plant fibers to develop new biodegradable materials is increasing quickly. In this context, nanocomposites reinforced with cellulose nanocrystals (CNCs) obtained from Bromelia (*Neoglaziovia variegate*) fibers have stood out as promising materials. Despite CNCs used to be separated from a cellulosic matrix in a good way with inorganic acids, the use of acidic ionic liquids (IL) has been arising as a safer and greener approach. Several authors have proposed the aprotic IL [BMIM][HSO_4] as an excellent alternative media to CNCs separation, and in previous work, we have proven that the cheaper protic IL [2-HEA][HSO_4] is valid for the same purpose. In this work, CNCs were separated from cellulose previously extracted from bromelia through the processing with H_2SO_4, [BMIM][HSO_4], and [2-HEA][HSO_4]. A variety of techniques, like thermogravimetric analysis (TGA), Fourier transform infrared (FTIR) spectroscopy, X-ray diffraction (XRD), electrophoretic light scattering (ELS), transmission electron microscopy (TEM) and atomic force microscopy (AFM) were used to CNCs characterization. The rod-like and spherical nanoparticles showed good thermal stability, and this could allow their incorporation into a polymeric matrix. Nanoparticles isolated with protic ionic liquid showed more excellent crystallinity when compared with nanoparticles with aprotic ionic liquid.

Keywords: Cellulose Nanocrystals. Ionic Liquid. Bromelia. Biodegradable Materials.

Introduction

With the concern and policies aimed at the environment, there has been great worldwide interest in developing technologies enabling products that cause less environmental impact [1].

In this context, vegetable fibers have been widely used as sources of cellulose nanocrystals (CNCs) to act as reinforcements in polymer matrices due to factors associated with cost, rigidity, renewability, abundance, and biodegradability [2-4]. *Neoglaziovia variegate* fibers are an excellent example of the mentioned characteristics and have a high cellulose content [5].

Received on 7 March 2023; revised 20 May 2023.
Ana Paula Bispo Gonçalves. Travessa São José 66 E, Arraial do Retiro, Cabula I. Zipcode: 40.000-000. E-mail: anapaulabisgon@gmail.com. DOI 10.34178/jbth.v6i2.293.

J Bioeng. Tech. Health 2023;6(2):124-132

CNCs are highly crystalline cellulose nanoparticles with a high aspect ratio (L/D) and are very rigid. It is necessary to remove the amorphous region of the cellulose by a hydrolysis reaction, maintaining the crystalline domains to obtain them [4,6]

They can act as reinforcement in polymeric matrices in small quantities, improving mechanical properties [7].

Hydrolysis from sulfuric acid is the best-known and widely used procedure. The method using aprotic ionic liquid to separate the crystalline phase of the amorphous region from cellulose is still little reported in the literature [8-10] and explores microcrystalline cellulose as a source.

However, the use of protic ionic liquid to obtain CNCs from renewable sources has not been reported in the literature. It can be an alternative to the aprotic ionic liquid since it can be synthesized easily, has a lower cost, and is safer, reusable, and less corrosive than inorganic solid acids [10]. Currently, ionic liquids have applications in treating biomass residues [11-14].

In this work, cellulose nanocrystals (CNCs) were obtained from bromelia (*Neoglaziovia variegate*) fibers from processing with sulfuric acid and ionic liquids: (1-butyl-3-methylimidazole hydrogen sulfate (aprotic) and 2-hydroxyethyl ammonium hydrogen sulfate (protic).

Using nanoparticles mixed with polymers has aroused interest in developing polymeric nanocomposites from CNCs, mainly from plant fibers, as reinforcement material for high-performance materials [15].

Other research route at stake for developing more environmentally friendly materials is the study of biodegradable polymers in detriment to those of complex degradation, whose main applications include sectors such as food packaging/ agriculture and the medical field [16-20].

The present study aims to separate and characterize CNCs from *Neoglaziovia variegate* fibers using conventional and alternative ways (ionic liquid processing).

Materials and Methods

Materials

Chemicals

Sulfuric acid (H2SO4), purity 95-99%, was supplied from Vetec and used to prepare the solution 55% (v/v). 1-butyl-3-methylimidazolium hydrogen sulfate ([BMIM][HSO_4]), purity > 95.0%, was supplied by Sigma-Aldrich and used as received without further purification. 2-hydroxyethyl ammonium hydrogen sulfate ([2-HEA][HSO_4]) ~30% (m/m) was synthesized from sulfuric acid and monoethanolamine, purity >90.0%, supplied by Neon.

Fibers

Bromelia fibers were collected in Araci, Bahia, Brazil. After washing, drying, and bleaching processes, the material was used to separate CNCs.

Methods

Separation of CNCs

$H2SO_4$ Processing

Bleached bromelia fibers were hydrolyzed at 50°C for 2 h under mechanical stirring at 1,150 rpm. For each gram of bleached material, 10 mL of H2SO_4(aq) 55% (v/v) was used. After the hydrolysis, 300 mL of water at 8°C was added to the system to quench the reaction. The resulting suspension was centrifuged several times to separate residual acid from precipitate, which was washed with distilled water at 4,400 rpm for 10 min to reach the CNCs dispersion in the water. The turbid suspension containing CNCs was submitted to dialysis for some days until pH 7 was reached [21,22]. Following this step, the purified suspension was stored in a refrigerator and named CNCSA (Cellulose Nanocrystals obtained with Sulfuric Acid).

Ionic Liquids Processing

Hydrolysis methodology was adapted with some modifications from [10]. Note that reaction conditions differ from H2SO_4 processing due to the specific physical features of the ILs, mainly viscosity, and acid strength. The reaction was performed in a becker at 70 C for 1,5 h under mechanical stirring at 580 rpm. For each gram of bleached material, 9 g of each IL was used separately. Following this step, 20 ml of water at 8°C was added to the system to quench the reaction. Centrifugation and dialysis were carried out in the same way described before. The purified aqueous suspensions containing CNCs were stored in a refrigerator and named CNCAPIL (Cellulose Nanocrystals obtained with Aprotic Ionic Liquid) and CNCPIL (Cellulose Nanocrystals obtained with Protic Ionic Liquid), respectively related to [BMIM][HSO_4] and [2-HEA][HSO_4].

Characterization

TEM, AFM, TG, FTIR, XRD, and Zeta potential characterized cellulose nanocrystals.

Transmission Electron Microscopy (TEM) was carried out in aqueous suspension, which was dripped onto 400 mesh copper grids covered with formvar film. Uranyl acetate solution 2 wt% was used as contrast. TEM micrographs were recorded in a JEOL microscope, model JEM-1230, operating at 80 kV, and Tecnai equipment, model G2-20. AFM micrographs were recorded in a Vecco e Cypher microscope, model Dimultimode V e ES Asylum Research. TG was performed in Shimadzu® equipment; model TG-A50 was analyzed from 25 to 800 °C at a heating rate of 20°C min^{-1} under a nitrogen flow of 100 mL min^{-1}. FTIR analysis was carried out using a Shimadzu spectrometer, model IR Prestige-21, transmittance mode, wavelength range of 4000-800 cm^{-1}. X-ray diffraction (XRD) was carried out in a Shimadzu X-ray diffractometer, model XRD-6000, angle range of 5°-50°. Dynamic Light Scattering (DLS) was conducted to determine the Zeta potential in a Zetasizer Nano ZS equipment with water at 25 °C.

Results and Discussion

Transmission Electron Microscopy (TEM)

A drop of each CNCs suspension was examined using TEM to confirm the separation of CNCs from bleached bromelia. Figure 1a shows CNCSA as rod-like nanoparticles, confirming them as cellulose nanocrystals. A bundle of particles is formed due to the preferential hydrogen bond formation between single nanoparticles instead hydrogen bonds with the hydrophobic substrate used to cover the cupper grid where the drop was added onto. Several other natural fibers, for instance, licorice, banana, palm; Calotropis procera, Macauba, and gravatar fiber, can provide similar rod-like CNCs [5], [23,24] that make separation of bundles of rod-like CNCs from 'caroá' with an aspect ratio of 16±5. The images of CNCAPIL and CNCPIL, both materials produced by ionic liquid processing, show nanoparticles with different shapes and sizes. While the first ones are rod-like, spherical morphologies were achieved using the protic ionic liquid.

Figure 1b shows that [BMIM][HSO_4] is an efficient medium to separate crystalline domains of cellulose (CNCs) from their amorphous domains under the tested conditions. The particle morphology of CNCAPIL is rod-like, as CNCSA, and all particles are on a nanometer scale, as reported by other authors [8,10]. Despite CNCSA and CNCAPIL being made both of rod-like nanoparticles, in CNCAPIL, the particles are less bonded to each other, which maybe a consequence of big ionic groups added into cellulose by [BMIM][HSO_4] over the reaction. Measurements of length, diameter, and aspect ratio of nanoparticles in image software are better to be done with single nanoparticles than a bundle of nanoparticles, suggesting an advantage for the use of ionic liquid processing [8] also successfully separated CNCS from microcrystalline cellulose using [BMIM][HSO_4] at 120 °C and 24 h of time reaction. The results presented in the current study and those from the literature suggest that [BMIM][HSO_4] improves energy and time-consuming reaction compared to $H2SO_4$ processing.

Figure 1c shows spherical nanoparticles for CNCPIL instead of rod-like morphology of CNCSA and CNCAPIL. The most probable reason to explain the spherical formation pathway under the conditions used for [2-HEA][HSO_4] processing is a self-assembly process of small cellulosic fragments around the rod-like nanoparticles during the drying. According to Lu and colleagues [25], self-assembly decreases particles' surface area, allowing a decrease in their free energy. [2-HEA][HSO_4] is probably inefficient in inserting charged groups on cellulosic chains so that particles can interact by the side by hydrogen bonds.

Table 1 shows the dimensions of CNCs, but CNCPIL measurements were impossible due to the difficulty of identifying the particles individually. On average, particle size for CNCSA was evaluated to be 252 nm in length and 20 nm in width, values which provided a high aspect ratio near to those reported by [24,26].

Figure 1. TEM images of CNCSA (a), CNCAPIL (b) and CNCPIL (c).

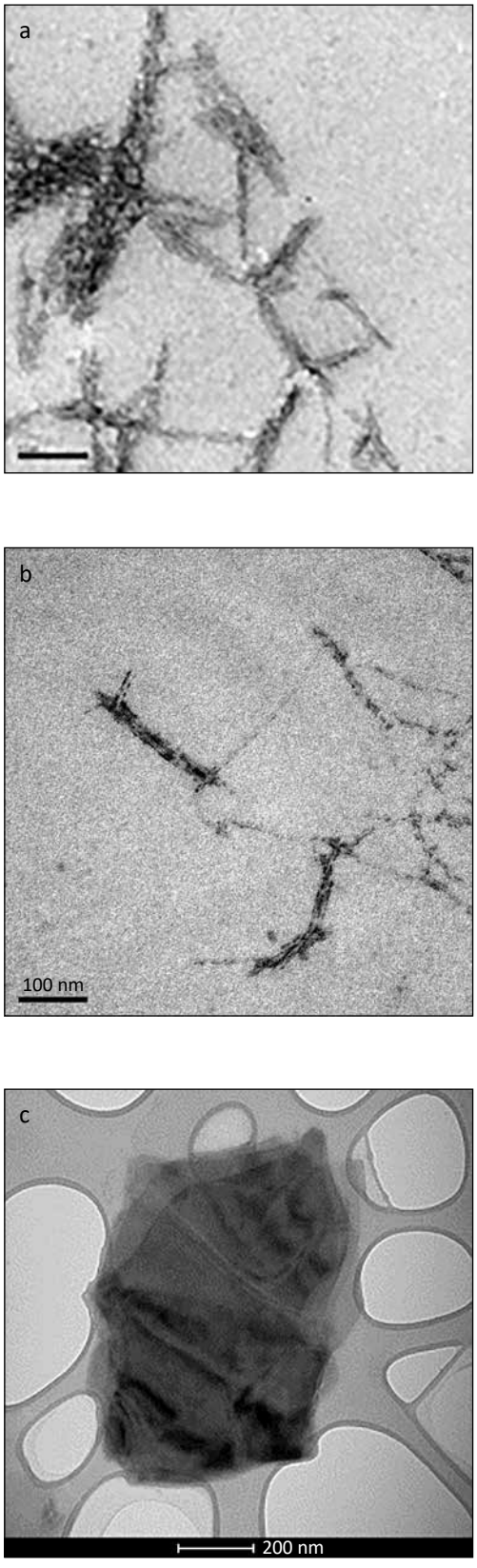

Tand and colleagues [10] found that processing of microcrystalline cellulose with [BMIM][HSO_4] at the temperature range of 70°C-100°C led to the formation of rod-like nanocrystals with diameters in the range of 15-20 nm and lower average aspect ratio than 28 (the average found in the current study – Table 1). It means the modifications made to the methodology of [BMIM][HSO_4] and the features of cellulose from bromelia fibers can provide CNCs with an aspect ratio fourfold. The massive importance of the aspect ratio of discontinuous phase (reinforcement) in nanocomposites comes from the percolation network between the phases at the interface, the zone responsible for the mechanical improvements achieved compared to the pure phases [27].

Nanostructures of high aspect ratios can strongly improve the mechanical properties of the matrix due to improvements in mechanical stress at the interfacial zone [28], so both CNCSA and CNCAPIL samples have the potential as mechanical reinforcements in nanocomposites.

Atomic Force Microscopy (AFM)

AFM measurements were carried out to confirm the particle size and morphology by other technique. Figure 2 shows AFM images of CNCs. Although no dissimilarities were observed when compared to TEM images - dimensions and morphology of CNCs were the same for both techniques. Figure 2c provides further details about the CNCPIL sample, which could not be apparent by TEM image: the spherical particles are made of small fragments. This observation agrees with the spherical pathway based on Gallardo-Sánchez and colleagues, and Lu and Lo Hsieh [29,30]. These results suggest that different mediums based on hydrogen sulfate anion allow the separation of different types of CNCs with a wide range of applications.

Electrophoretic light scattering (ELS)
It is not enough to separate CNCs from a cellulosic source; they must keep their dimensions on the nanometer scale. ELS measurements

Table 1. Length, diameter, and aspect ratio of CNCs.

Sample	Length (nm)	Diameter (nm)	Aspect Ratio
CNCSA	252.00 ± 127.94	20.00 ± 14.56	35.09 ± 29.73
CNCAPIL	147.39 ± 60.82	5.55 ± 2.81	27.97 ± 3.87

were carried out to evaluate the stability of suspensions. The negative values of Zeta potential for all samples confirm the presence of negatively charged groups at the surfaces of CNCs over the reaction, such as sulfate and hydrogen sulfate. According to the electrostatic model, the electrostatic repulsion between particles charged with the same signal is the main reason to keep the nanoparticles isolated and stabilized by water molecules. So, as much negative, the Zeta potential is, the more stable the sample is. According to the literature [29], [31] ideal suspensions with Zeta potential higher than 30 mV must be stable so CNCs do not tend to aggregate into more considerable microscopic fragments. Based on the values shown in Table 2, none of the samples meet the stability criteria; however, the values agree with those found by other authors. [29]. CNCPIL was the less stable suspension, and this result deals with the discussion about spherical pathway formation in this sample.

Figure 2. AFM images of CNCSA (a), CNCAPIL (b) and CNCPIL (c).

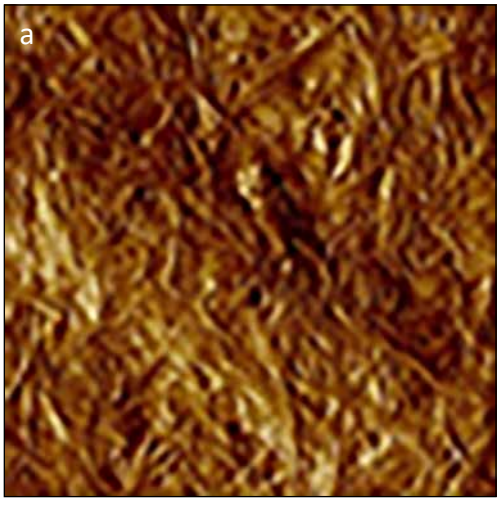

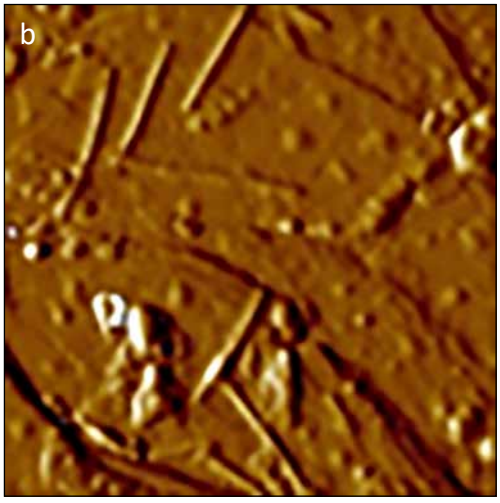

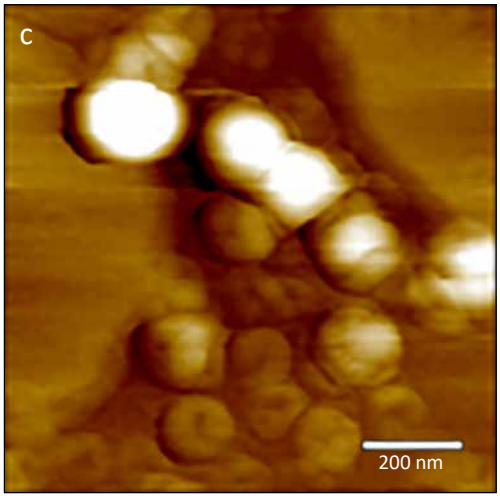

Thermogravimetric Analysis (TGA)

Thermal degradation of cellulose involves chemical reactions such as depolymerization, dehydration, and decomposition of glycosyl units, processes strongly dependent on the surface area of particles and the charged surface groups. TGA measurements were carried out to evaluate the

Table 2. Potential zeta of CNCs.

Sample	Zeta Potential (mV)
CNCSA	-21.1 ± 0.5
CNCAPIL	-23.5 ± 0.4
CNCPIL	-20.3 ± 0.2

thermal behavior of each sample and understand the influence of each kind of processing (Figure 3). Sample CNCSA was thermally stable until 232°C, with a weight loss of 3 %. DTG profile shows two events: the first at a maximum temperature of 55°C related to humidity loss [32], and the second related to the degradation of sulfated cellulose present on the surface of CNCs. These regions are more susceptible to thermal degradation when compared to the uncharged bulk. Sample CNCAPIL was thermally only until 214°C. DTG profile shows three events: Besides the events related to moisture (below 100°C) and degradation of sulfated cellulose by pyrolysis (214-380°C with maximum degradation temperature until 306°C) [9,32], a third event above 600 °C appears related to carbonaceous matter [24]. This event is absent in CNCSA because of the abundance of sulfated groups over the surface.

CNCPIL was the less thermally stable sample, holding on until 205ºC. DTG profile shows the same three events (at 70-100ºC, 205-389ºC, and 684-773ºC) already discussed for CNCAPIL. Despite the less charged surfaces for CNCPIL, AFM images suggest smaller particles when compared to CNCSA and CNCSAPIL, so small particles tend to have a higher specific surface area, increasing the exposure area over the heating. However, the thermal stability of CNCPIL is enough to allow its incorporation at formulations based on thermoplastic matrices because the most usual range of processing temperature for these materials is around 200°C [33].

Fourier transform infrared spectroscopy (FTIR)

FTIR measurements were carried out to confirm the presence of sulfate groups at the surface of CNCs and their nature of water affinity. Figure 4 shows FTIR spectra of all samples. The signal at 1620 cm^{-1} is related to adsorbed water vapor and is present in all curves, suggesting a hydrophilic nature [10,32]. The signal at 11631 cm^{-1} is attributed to S=O vibration. This double bond belongs to sulfate groups and is present in all curves. All processing methodologies effectively separate and stabilize the CNCs by esterifying their surfaces with sulfate groups.

X-ray Diffraction (XRD)

XRD measurements were carried out to evaluate each sample's crystallinity using the Crystallinity

Figure 3. TGA (a) and DTG (b) profiles of CNCs.

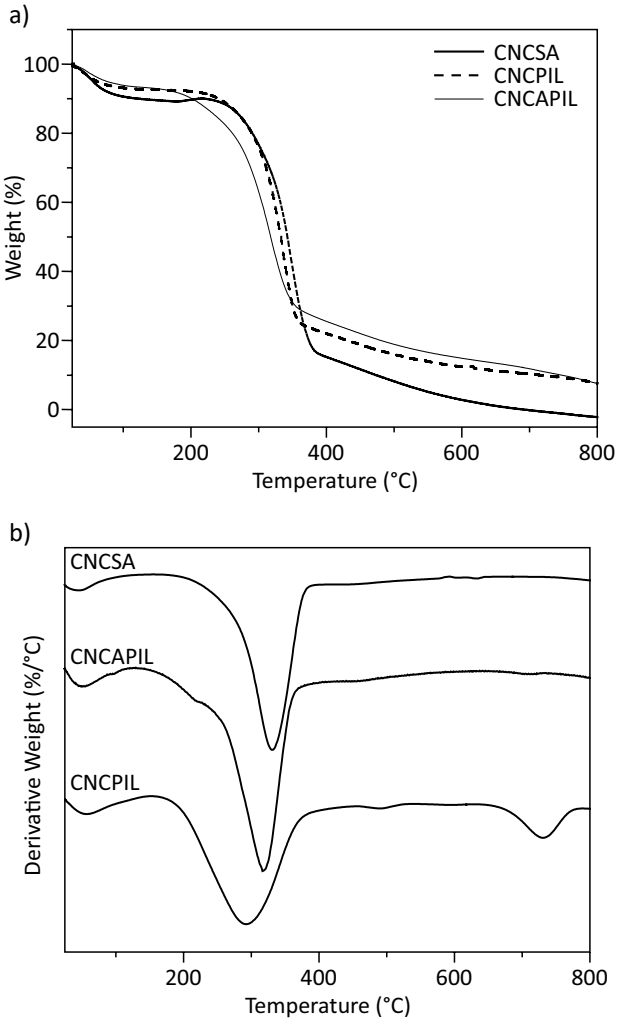

Figure 4. FTIR spectra of CNCSA (a), CNCAPIL (b) and CNCPIL (c).

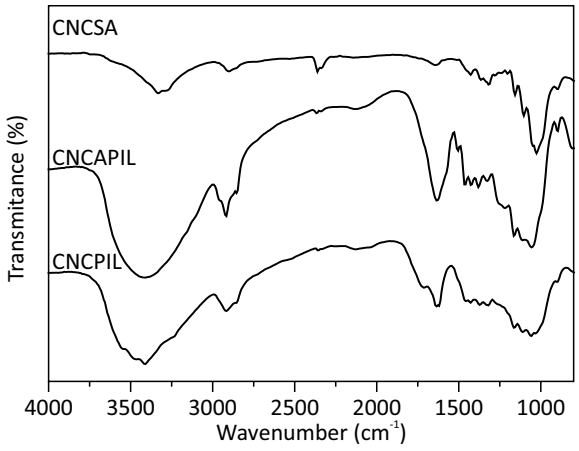

Index (C.I.) approach, aiming to understand the influence of the processing methodologies employed. Figure 5 presents the results.

Diffraction peaks at 2Θ=15, 22, and 34° ((110), (200), and (040) plans, respectively) are assigned to the suitable cellulose I [34] and are present in the XRD profile of CNCSA. The high intensity of the peak at 22° contributes to the highest C.I. of samples, around 76%. This result suggests the extraordinary ability of the sulfuric acid solution to provide hydronium ions able to break glycosidic bonds from amorphous cellulose and release single CNCs. XRD profiles of CNCAPIL and CNCPIL also exhibit diffraction peaks typical of cellulose I ((110) and (200) plans) [10,35], suggesting that ionic liquid processing methodologies employed were suitable to avoid the cellulose interconversion to unsuitable II types. However, it is essential to highlight the low C.I. calculated for CNCAPIL and CNCPIL because it suggests some degradation and crystalline parts of cellulose, as already noted by Tand and colleagues and Haron and colleagues [10,13]. It could be explained based on the swelling ability of ionic liquids, so their cations can migrate between cellulosic chains, separating them and changing the spatial configuration to some extent. The results of XRD are in good agreement with TGA and FTIR results.

Figure 5. XRD profiles of CNCSA (a), CNCAPIL (b), and CNCPIL (c).

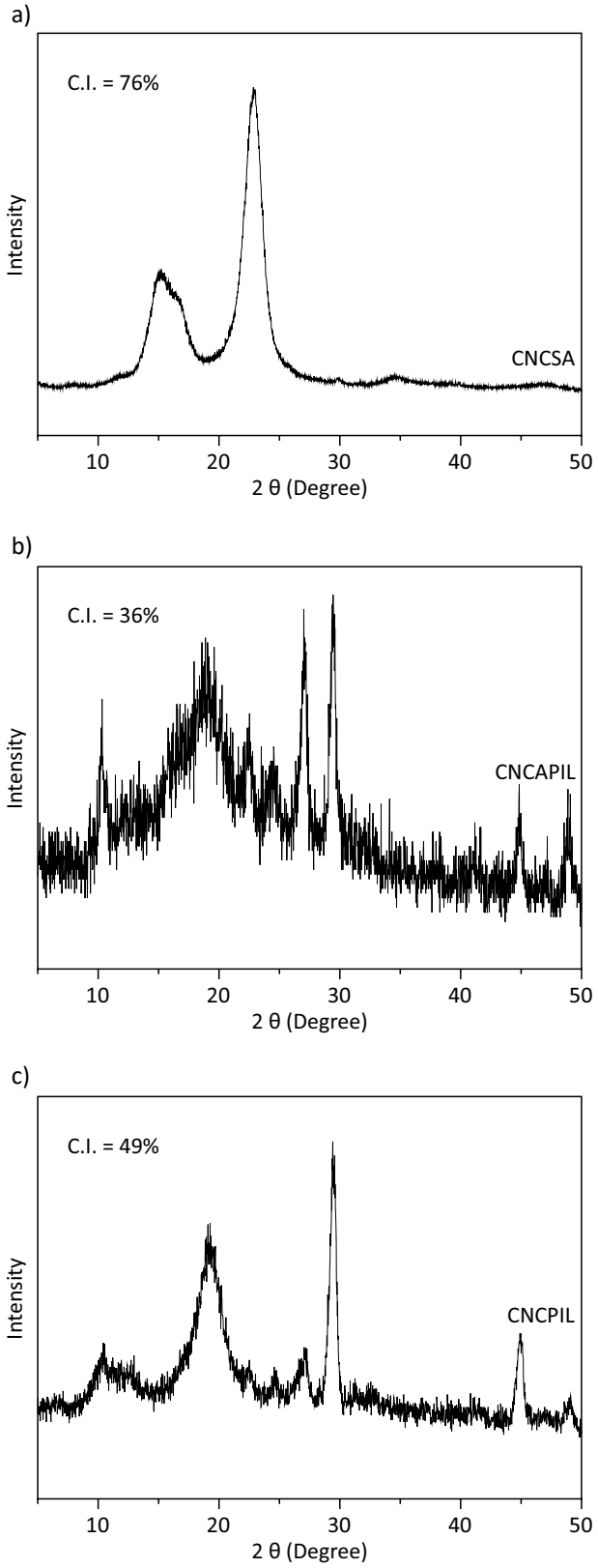

Conclusion

From the use of the sulfuric acid solution, [BMIM][HSO_4] and [2-HEA][HSO_4], it was possible to separate the cellulose crystalline regions of bromelia (*Neoglaziovia variegate*) fibers from the amorphous phase, obtaining cellulose nanoparticles with shaped and spherical shapes, as shown in the TEM and AFM analyzes. The spherical shape obtained from protic ionic liquid can provide important characteristics in new applications that can be studied. Protic ionic liquid has the advantages of being less corrosive than sulfuric acid, capable of reuse, and less costly and less toxic compared to aprotic, being, therefore, a new alternative in obtaining cellulose nanocrystals to be used explored. The CNCSA sample was more thermally stable when compared to the CNCAPIL and CNCPIL samples, showing a higher crystallinity index. CNCPIL also presented a higher crystallinity index when compared to CNCAPIL. The good thermal stability of the three types of CNCs makes it possible to use them in material processing, such as extrusion, and thus could be used as reinforcement to a biodegradable matrix, enhancing the range of possible applications for these materials.

Acknowledgment

The authors would like to thank FAPESB and CAPES for financial support and Fiocruz-BA, LAMUME-UFBA, and UFMG for characterization techniques. We also thank to the financial support of CNPq (Grant PQ 306640/2016-3).

References

1. Schreiber D, Ermel UT, Figueiredo JAS, Zeni A.Analysis of innovation and its environmental impacts on the chemical industry. BAR - Brazilian Administration Review 2016;13(1):56–75. doi: 10.1590/1807-7692bar2016150120.
2. Gazzotti s et al. Polylactide/cellulose nanocrystals: The *in situ* polymerization approach to improved nanocomposites. Eur Polym J 2017;94:173–184. doi: 10.1016/j.eurpolymj.2017.07.014.
3. Youssef AM, El-Sayed SM, Salama HH, El-Sayed HS, Dufresne A. Evaluation of bionanocomposites as packaging material on properties of soft white cheese during storage period. Carbohydr Polym 2015;132:274–285. doi: 10.1016/j.carbpol.2015.06.075.
4. Doan TKQ, Chiang KY. Characteristics and kinetics study of spherical cellulose nanocrystal extracted from cotton cloth waste by acid hydrolysis," Sustainable Environment Research 2022;32(1). doi: 10.1186/s42834-022-00136-9.
5. Gonçalves AP, Oliveira E, Mattedi S, José NM. Separation of cellulose nanowhiskers from microcrystalline cellulose with an aqueous protic ionic liquid based on ammonium and hydrogensulphate. Sep Purif Technol 2018;196:200–207. doi: 10.1016/j.seppur.2017.07.054.
6. Hassanzadeh-Aghdam MK, Ansari R, Darvizeh A. Micromechanical analysis of carbon nanotube-coated fiber-reinforced hybrid composites. Int J Eng Sci 2018;130:215–229. doi: 10.1016/j.ijengsci.2018.06.001.
7. George J, Sabapathi SN. Cellulose nanocrystals: Synthesis, functional properties, and applications. Nanotechnol Sci Appl 2015;8:45–54. doi: 10.2147/NSA.S64386.
8. Mao J, Osorio-Madrazo A, Laborie MP. Preparation of cellulose I nanowhiskers with a mildly acidic aqueous ionic liquid: Reaction efficiency and whiskers attributes. Cellulose 2013;20(4):1829–1840. doi: 10.1007/s10570-013-9942-2.
9. Man Z, Muhammad N, Sarwono A, Bustam MA, Kumar MV, Rafiq S. Preparation of cellulose nanocrystals using an ionic liquid. J Polym Environ 2011;19(3):726–731. doi: 10.1007/s10924-011-0323-3.
10. Tan C et al. Role of surface modification and mechanical orientation on property enhancement of cellulose nanocrystals/polymer nanocomposites. Eur Polym J 2015;62:186–197. doi: 10.1016/j.eurpolymj.2014.11.033.
11. Bandara TR, Griffin GJ. Transport of sugars contained in an ionic liquid medium via a supported liquid membrane. Journal of Ionic Liquids 2022;2(1):100026. doi: 10.1016/j.jil.2022.100026.
12. Bagh FSG, Ray S. Lignin extraction from black liquor using acetate based ionic liquids: Extraction kinetics and product characterization. Journal of Ionic Liquids 2022;2(1):100028. doi: 10.1016/j.jil.2022.100028.
13. Haron GAS, Mahmood H, Noh MH, Alam MZ, Moniruzzaman M. Ionic Liquids as a sustainable platform for nanocellulose processing from bioresources: Overview and current status. ACS Sustain Chem Eng 2021;9(3):1008–1034. doi: 10.1021/acssuschemeng.0c06409.
14. Jisha KJ, Rajamani S, Singh D, Sharma G, Gardas RL. A comparative study of ionothermal treatment of rice

straw using triflate and acetate-based ionic liquids," Journal of Ionic Liquids 2022;2(2):100037. doi: 10.1016/j.jil.2022.100037.
15. Ilyas Rushdana A, Sapuan Salit M, Lamin Sanyang M, Ridzwan Ishak M. Nanocrystalline cellulose as reinforcement for polymeric matrix nanocomposites and its potential applications: A review. Curr Anal Chem 2017;13. doi: 10.2174/1573411013666171003155624.
16. Yuvaraj D et al. Advances in bio food packaging – An overview. Heliyon 2021;7(9). doi: 10.1016/j.heliyon.2021.e07998.
17. Milani P, França D, Balieiro AG, Faez R. Polymers and its applications in agriculture. Polimeros 2017;27(3):256–266. doi: 10.1590/0104-1428.09316.
18. Nofar et al. Mechanical and bead foaming behavior of PLA-PBAT and PLA-PBSA blends with different morphologies. Eur Polym J 2017;90:231–244. doi: 10.1016/j.eurpolymj.2017.03.031.
19. Palsikowski PA, Roberto MM, Sommaggio LRD, Souza PMS, Morales AR, Marin-Morales MA. Ecotoxicity Evaluation of the Biodegradable Polymers PLA, PBAT and its Blends Using Allium cepa as Test Organism. J Polym Environ 2-18;26(3):938–945. doi: 10.1007/s10924-017-0990-9.
20. Hema Prabha P, Ranganathan TV. Process optimization for evaluation of barrier properties of tapioca starch based biodegradable polymer film. Int J Biol Macromol 2018;120:361–370. doi: 10.1016/j.ijbiomac.2018.08.100.
21. de Miranda CS. Desenvolvimento de bionanocompósitos a partir de nanowhiskers de celulose da fibra de gravatá e lignina na matriz de amido e PBAT/amido. 2015, [Online]. Available: https://repositorio.ufba.br/ri/handle/ri/19523.
22. da Silva JBA, Pereira FV, Druzian JI. Cassava starch-based films plasticized with sucrose and inverted sugar and reinforced with cellulose nanocrystals. J Food Sci 2012;77(6):. doi: 10.1111/j.1750-3841.2012.02710.x.
23. Song K, Zhu X, Zhu W, Li X. Preparation and characterization of cellulose nanocrystal extracted from Calotropis procera biomass. Bioresour Bioprocess 2019;6(1). doi: 10.1186/s40643-019-0279-z.
24. Carneiro J, Oliveira DE. Síntese e Caracterização de nanocompósitos poliméricos reforçados com whiskers de cellulose da fibra de licuri. Universidade Federal da Bahia, Escola Politécnica, Programa de Pós Graduação em Engenharia Química, 2015.
25. Lu H, Gui Y, Zheng L, Liu X. Morphological, crystalline, thermal and physicochemical properties of cellulose nanocrystals obtained from sweet potato residue. Food Research International 2013;50(1):121–128. doi: 10.1016/j.foodres.2012.10.013.
26. Martins MA, Teixeira EM, Corrêa AC, Ferreira M, Mattoso LHC. Extraction and characterization of cellulose whiskers from commercial cotton fibers. J Mater Sci 2011;46(24):7858–7864. doi: 10.1007/s10853-011-5767-2.
27. Dufresne A. Cellulose nanomaterial reinforced polymer nanocomposites. Current Opinion in Colloid and Interface Science 2017;29:1–8. doi: 10.1016/j.cocis.2017.01.004.
28. Klemm D et al. Nanocelluloses: A new family of nature-based materials," Angewandte Chemie - International Edition 2011;50(24):5438–5466. doi: 10.1002/anie.201001273.
29. Gallardo-Sánchez MA et al. Optimization of the obtaining of cellulose nanocrystals from agave tequilana weber var. Azul Bagasse by acid hydrolysis. Nanomaterials 2021;11(2):1–21. doi: 10.3390/nano11020520.
30. Lu P, Lo Hsieh Y. Cellulose isolation and core-shell nanostructures of cellulose nanocrystals from chardonnay grape skins. Carbohydr Polym 2012;87(4):2546–2553. doi: 10.1016/j.carbpol.2011.11.023.
31. Duffy JJ, Panalytical M, Hill AJ. Suspension stability; Why particle size, Zeta potential and rheology are important. 2012. [Online]. Available: https://www.researchgate.net/publication/279851764.
32. Trilokesh C, Uppuluri KB. Isolation and characterization of cellulose nanocrystals from jackfruit peel. Sci Rep 2019;9(1). doi: 10.1038/s41598-019-53412-x.
33. Flauzino, Neto, WP, Silvério HA, Dantas NO, Pasquini D. Extraction and characterization of cellulose nanocrystals from agro-industrial residue - Soy hulls. Ind Crops Prod 2013;42(1):480–488. doi: 10.1016/j.indcrop.2012.06.041.
34. Ju X, Bowden M, Brown EE, Zhang X. An improved X-ray diffraction method for cellulose crystallinity measurement. Carbohydr Polym 2015;123:476–481. doi: 10.1016/j.carbpol.2014.12.071.
25. Sheltami RM, Abdullah I, Ahmad I, Dufresne A, Kargarzadeh H. Extraction of cellulose nanocrystals from mengkuang leaves (*Pandanus tectorius*). Carbohydr Polym 2012;88(2):772–779. doi: 10.1016/j.carbpol.2012.01.062.